PHYSICAL MODEL OF KEROSENE PLUME MIGRATION IN AN UNSATURATED ZONE OF THE SANDY SOIL

Prof. Dr. Rafa H. Al-Suhaili
University of Baghdad
College of Engineering

Hussein A. M. Al -Madany
University of Kufa
College of Engineering

ABSTRACT

Physical model tests were simulated non-aqueous phase liquid (NAPL) spill in two-dimensional domain above the water table. Four laboratory experiments were carried out in the sand-filled tank. The evolution of the plume was observed through the transparent side of this tank and the contaminant front was traced at appropriate intervals. The materials used in these experiments were Al-Najaf sand as a porous medium and kerosene as contaminant.

The results of the experiments showed that after kerosene spreading comes to a halt (ceased) in the homogeneous sand, the bulk of this contaminant is contained within a pancake-shaped lens situated on top of the capillary fringe.

موديل فيزيائي لحركة كتلة النفط الأبيض في المنطقة غير المشبعة من التربة الرملية

الخلاصة

لقد تضمن العمل المختبري تمثيل تسرب السائل العضوي الأخف من الماء في الطبقة ذات البعدين فوق مستوى الماء الجوفي. حيث اجريت اربعة تجارب مختبرية في حوض زجاجي صنع لهذا الغرض وملأ بالرمل. ان استخدام الزجاج يوفر الأمكانية المطلوبة لمتابعة تقدم مقدمة الملوث وبالتالي رسم شكلها خلال فترات زمنية مختلفة. لقد تم اختيار تربة مدينة النجف لتمثيل الوسط المسامي في كل التجارب المختبرية الحالية في حين تم اختيار النفط الأبيض لتمثيل السائل العضوي المتسرب إلى ذلك الوسط.

أظهرت التجارب المختبرية للترب المتجانسة عند توقف انتشار الملوثات النفطية فان كمية كبيرة من الملوثات سوف تشكل شكلا مفلطحا مستقرا فوق منطقة capillary fringe.

INTRODUCTION

The problem of evaluating the factors controlling the movement of Non-Aqueous phase Liquids ($NAPL_s$) in shallow subsurface has received increasing attention in the last decade after a number of sites throughout the United States have been found to be contaminated with organic chemicals, mostly petroleum products (McKee et al., 1972; Kramer, 1982), aromatic compounds (Oliveira and Sitar, 1985) and halogenated hydrocarbons. Once a NAPL is released into the subsurface, it continues to travel as a separate liquid phase until it becomes immobile. When the migration of the NAPL reaches its final stage, this contaminant remains as isolated ganglia or pools. These pools act as a source of further contamination by dissolution and vaporization.

Soil and ground water contamination by ($NAPL_s$) such as organic solvents, gasoline and other petroleum products is widespread due to leaking storage tanks, spills, and improper disposal processing. Although $NAPL_S$ are relatively immiscible with water, understanding the behavior of these liquids in the subsurface is important since solubility may exceed drinking water standards. After release, NAPL migrates as a separate phase downward by gravity with some lateral spreading due to capillary forces. If sufficient NAPL has been spilled, eventually, it may reach the groundwater surface. If it is lighter than water (LNAPL) it will accumulate as a liquid mound that floats on the ground water surface. If it is denser than water (DNAPL) it displaces ground water and continues downward migration until it encounters a hydraulic or capillary barrier as shown in Fig. 1. Floating LNAPL can partly be removed by creating a pumping well (Mercer and Cohen, 1990). The LNAPL will flow towards the well facilitated by the groundwater table gradient and can be pumped into a recovery tank. Although removing DNAPL is more difficult task, DNAPLs can be pumped out of the subsurface. Not all of the NAPL can be removed, since some of it is retained in the capillaries of the porous medium. This remaining NAPL can be contained hydrologically or can be removed by other techniques such as air sparging or bioremediation. To predict the NAPL that was left behind in the unsaturated zone after remediation by pumping, the mechanisms that are responsible for the flow and retention of NAPL must be understood. Therefore, such understanding is a major motive for studying the movement, interaction and distribution of three fluid phases, i. e., water, NAPL and air in a porous medium: the subsurface.

The unsaturated zone is a multiphase system, consisting of at least three phases: a solid phase of the soil matrix, a gaseous phase and the water phase (Bear, 1972). Additional phase may also be present such as a separate phase organic liquid. Oil properties such as density, viscosity, interfacial tension, solubility and vapor pressure are important in understanding oil transport and in predicting subsurface contamination.

Al Najaf is one of the most important cities in Iraq. It is the spiritual center of all Moslems because the holy shrine of Al Imam Ali. It is located on high plateau over a sandy ground (Al Shakerchy, 2007). Al Najaf is expected to have a huge development program in the coming years through the construction of many gasoline stations, chemical manufacturing and processing plants and other facilities for storing hazardous materials has led to the installation of underground storage tanks (USTs). Many of installed (old) tanks have exceeded or are currently close to the end of their useful life and are now (or will soon be) leaking, posing a serious threat to soil and groundwater quality as well as to public health and welfare. To establish the most effective soil remediation technology that can be utilized in the control of releases from leaking UST_S and to minimize unreasonable risks to human health and the environment, it is essential to identify likely

contaminants and the severity of contamination from leaking UST_S, therefore, Al Najaf sand soil was used here in the experimental works to represent an actual case.

PHYSICAL MODEL

Sand Tank

The sand tank model was built to study the movement of the (LNAPL) in the vadose zone. The simulated spills were performed in a tank 71cm long, 61cm high, and 5cm wide, schematically shown in Fig. 2. Pressure ports and electrodes locations are shown in Fig. 3. The front side of the tank was transparent to allow for visual observations. It consisted of a glass plate for the initial experiments and was later replaced by a Lucite plate in order to accommodate for the design adopted for the saturation measurements. Two pairs of metal reinforcing bars were clamped on the exterior of the tank to prevent bending of the more deformable Lucite plate. The back side of the tank made of stainless steel, was designed to be removable to allow for measurement of the extent of the plume at the back and for examination of the contaminated area within the sample by careful dissection at the end of each experiment. Two vertical perforated stainless steel partitions, covered with stainless steel mesh, provided the lateral boundaries of the sand-filled middle compartment, which had dimensions 61x 61 x 5cm. The purpose of the two outer compartments was to provide constant head reservoirs for controlling the position of the water table within the sand deposited in the middle and, in addition, to control the wetting and drainage of the sand mass.

Materials

A) Soil: Two sizes of available sand, designated #14 (coarse) and #50 (fine), were used for the experiments which brought from Al-Najaf city/Al Adala Quarter. Additional sieving was necessary to achieve satisfactory uniformity. The sand was also washed to remove fine particles and salts which if dissolved into the water-NaCl solution would alter its electrical properties, as discussed above. The result of the grain size distribution, as shown in Fig. 4, shows that the soil is consisting about of 2.66% gravel, 96.6% sand, and about 0.7% fine. The characteristics of the grain distribution curve give the uniformity coefficient, (C_u) =8.67 and the coefficient of gradation, (C_c) =1.35. According to unified soil classification system, the soil was classified as well graded (Das, 1985). The median grain size of the soil is 0.9 mm.

B) Contaminant Liquid: After considering various organic liquids, kerosene was chosen as the contaminant fluid. The selection was based on the low health hazard of kerosene during experiment, in combination with a number of desirable properties such as specific gravity lower than 1.0, viscosity comparable to that of water, very low solubility in water, and low volatility. The last two properties are necessary to limit the mass transfer between phases during the experiments. The pertinent properties of kerosene are summarized in Table (1). In order to enable visual observations, kerosene was dyed with Sudan III. “Sudan” is trade mark (or name) for a line of dyestuffs, soluble in hydrocarbons; used for the coloring of fats, oils, waxes….etc. Sudan III is a powdered, nonvolatile an organic dye of red color which is insoluble in water.

* SAMPLE PREPARATION

The tests were conducted in a constant temperature room (21°C) which is necessary for such experiments, since electrical properties, and to lesser extent, surface properties are temperature dependent. Sand was then deposited in lifts by dry pluviation. Since uniform sands were used, special packing procedures were not deemed necessary in order to achieve homogeneous samples. The soil density used here is 1.128 gm/cm^3 for coarse sand and 1.026 gm/cm^3

for fine sand. Before the last lift was placed in the tank a Lucite cylinder, which served as the source of the kerosene, was embedded in the center of the top of the sample and filled with sand to the same final height as the rest of the sample (Fig. 2). The inside diameter of the cylinder was 3.2 cm. The final height of the samples ranged between 49 and 52 cm.

After all the sand was in place, water was slowly introduced via the outer compartments, to form a water table 3-4 cm above the bottom of the tank. More water was permitted to flow from the reservoirs connected to the tank through the outer compartments and into the sample to maintain the water table at the same height, as water infiltrated into the sand due to capillary rise. When the water table stabilized, i.e. when imbibitions of water into the sand ceased, the water table was raised another 3-4 cm, and the same procedure was repeated until the water table finally equilibrated at the top of the sample. The wetting rate was kept slow in order to achieve the maximum water saturation possible while relying only on moistening by capillarity. Wetting of the samples typically lasted 2-3 hours and resulted in water saturation close to 85%.

After the sample was wetted, drainage was initiated by lowering the water table in the outer compartments to the desired height, typically 4 and 16 cm above the base of the tank for the fine and coarse sand, respectively. The two different water table elevations compensated for the different extent of the capillary fringe in the two sands. The samples were allowed to drain overnight, for at least 12 hours. After drainage was completed, three distinct regions appear above the water table. The first is the capillary fringe where there is maximum water saturation under negative pressure. The second zone is the visibly wet area above the capillary fringe where water saturation decreases with increasing distance from the water table. Finally, the third zone is visibly dry (although still moist) region at the top apparently corresponds to the zone where water is discontinuous.

* TEST PROCEDURE

Each experiment began by introducing kerosene inside the cylinder which simulated a leaking underground facility in the sand tank model. In all experiments, a total of 350 cm^3 of kerosene was used, equal to approximately 10% of the pore space above the capillary fringe. Kerosene was added as needed to maintain the height of the free liquid inside the cylinder always at 4 cm above the top of the sand, until all of 350 cm^3 of kerosene were used. The rate at which kerosene was added to adjust the level at 4 cm was dictated by the rate at which kerosene from the cylinder disappeared into the sand. In this way, in all the experiments kerosene infiltrated under a constant head. The plume was traced at appropriate intervals during both the infiltration (while the source of leak is active) and the redistribution (when no additional kerosene enters the sample) stages, until no significant changes of the front were observed.

Water volume flowing out of the tank was measured and kerosene front was traced (Figs. 4 and 5) at the appropriate intervals. The development of the plume was typically monitored for 24 hours, well after any visible movement of the front had ceased. At the completion of the experiment, the tank was tilted and the back plate was removed in order that the final position of the contaminant front on the back side could be traced. The samples were subsequently dissected, so as to examine the distribution of kerosene in the sand.

A central area which was uniformly contaminated with kerosene was invariably observed, beyond this area, interconnected pockets of kerosene were found which extended to the boundaries of the front as observed through the Lucite plate, indicating minimal boundary effects. A total of 4 simulated spills were performed in homogeneous sands. More specifically, two experiments were conducted with fine sand (#50) and the other experiments with coarse sand (# 14).

* VISUAL OBSERVATION

The experiments with homogeneous coarse (#14) and fine (#50) sands showed that although kerosene infiltrates more rapidly in the coarse sand, the evolution of the contaminant front follows similar patterns despite differences in grain size, provided that the top of the capillary fringe at the same elevation. At the initial stage of the spill, the front retains a regular, circular shape, after few times the front shape becomes ellipsoid as it advances (Figs. 5 and 6). After the contaminant front reaches the boundary between visibly wet dry sand its shape becomes irregular and is characterized by fingering and lateral spreading, as was also reported by Schwille (1984).

When kerosene becomes immobilized and spreading ceases, the final contaminated area consists of two distinct regions, an elongated, pancake-shaped area of high kerosene saturation and the area above it, which was previously swept by the front, at residual kerosene saturation. The top of the kerosene-wet area was slightly above the visibly wet–dry sand boundary in all experiments. The maximum horizontal extent of the kerosene lens occurred at an elevation close to and below the visibly wet-dry sand boundary. Thickness of this pancake- shaped lens was consistently higher in the fine sand.

EXPERIMENTAL RESULTS

A) Propagation of the Contaminant Front: To quantify the information obtained from the simulated spills, the development of the contaminant front with time was described by the following variables: the volume of kerosene in the sample, the volume of the sample which was contaminated by kerosene, the average kerosene saturation in the contaminated zone, the distance between the lowest point of the front and the water table, and the distance between the source of the leak and the front. The values of these parameters for the fine (#50) and coarse (#14) sands are listed in Table 2. The extent and the geometry of the final contaminant front were described by the variables listed in Table 3, the percentage of the total volume of the sample which was contaminated by kerosene, the ratio of the volume of contaminated soil to the total volume of the contaminant liquid spilled, and the lens thickness.

A comparison of data for the two sands (Table 2) shows that the final vertical extent of the plume (distance from the leak) is the same for both sands as a result of the same capillary fringe elevations, although the total contaminated area is larger for the fine sand. More specifically, a comparison of the parameters describing the final position of the front (Table 3) shows that the average percentage of the total sample volume contaminated by kerosene is 21.14% for the fine sand, dropping to 19.34% for the coarse sand. Thus the ratio of the kerosene-contaminated sand to the infiltrated kerosene volume is 10.50 in the fine sand and 7.59 in the coarse sand. Kerosene saturation remained consistently lower in the fine sand during all stages of the test, apparently due to the higher initial water saturation in the fine sand, as will be discussed later.

The spreading rate of the contaminant front during kerosene infiltration was also computed from the mean values of the kerosene-contaminated area for the two sands. Spreading rate was calculated based on new volume swept by the front during a time interval (dV/dt), as well as on total volume swept at a time measured from the beginning of infiltration divided by this time (V/t). The two rates are very similar to each other for the same sand, indicating that the spreading rate remains constant during infiltration. The mean values were 18.80 and 86.95 cm^3/min for the fine and coarse sand, respectively.

B) Measurement of Phase Variables: The measurements obtained during two of the experiments, with homogeneous fine and coarse sand, are presented here to illustrate the observed changes in water saturation and the pressure head response. The water table was lowered to 3.9 and 16.0 cm from the

bottom of the tank for the fine and the coarse sand, respectively. Subsequent drainage lasted 14 hours for the fine sand and 12 hours for the coarse sand. At the end of this period water pressures and saturations were changing at a very slow rate indicating that static equilibrium above water table was achieved. Following drainage, a total of 350 cm^3 of kerosene was allowed to infiltrate through the Lucite cylinder simulating the leaking facility under a constant head of 4 cm. After all the kerosene was used, infiltration continued under a declining head until all kerosene was in the sand mass and redistribution started. A summary of the two tests is given in Table 4, which also includes the volume of the water that flowed out of the tank during the kerosene infiltration stage.

DISCUSSION

The data from the fully instrumented tests confirm and explain the visual observation regarding the characteristics of the advancing plume and its final extent. On the basis of the visual observations of the kerosene front, it was found that the ratio of spreading rates during infiltration for the coarse and fine sand (86.95/18.8=4.6), the ratio of kerosene of infiltration rates was twice as high (21.6/2.9=7.4). These results can be explained by considering the different saturation profiles for the two sands. Although the top of the capillary fringe (area of maximum saturation) in both samples is located at the same elevation, the saturation distribution above it is dissimilar due to differences in grain size distribution (higher uniformity in the coarse sand produced a flatter capillary pressure curve).

In order to move downward, kerosene has to displace more water in the fine sand than in the coarse sand, as evidenced by the higher saturation changes during infiltration in the fine sand samples and by the larger volume of water displaced at the end of the infiltration stage, 275 cm^3 for the fine sand compared to only 145 cm^3 for the coarse sand. However, while vertical movement is delayed in the fine sand, kerosene moves laterally. As a result, although in both cases the kerosene front extends over the same vertical distance 21.7 cm and 22.9 cm for the coarse and fine sand, respectively, the total contaminated area is wider in the fine sand. Again, as a consequence of the different water saturation distribution, as determined from the capillary pressure-saturation curves of the two sands, the final average kerosene saturation is lower for the fine sand.

The results of the comprehensive analysis in Al Najaf city sand (especially for gypsum content) showed that there are two main categories with respect to the changing with depth, first, at depth range of 0.5-2.0m, and second, at depth range of 2.0-12.5m, where at first range, the content of gypsum changes randomly from area to another, so, the average value of gypsum content range of 18-24.19 %. At depth range of 2.0-12.5m, the gypsum content ranged of ≤6 % (Al Shakerchy, 2007). When gypseous soils are irrigated, the gypsum is leached and then located and in some cases a gypsum layer is formed which reduces the hydraulic conductivity. This will decreasing trend of contaminant movement.

CONCLUSIONS

The following conclusions are drawn on the basis of the results obtained from the present experimental measurements:

a) Visual observations from the sand tank model show that the front retains an elliptic shape during the final stages of infiltration, but later on, as it approaches the capillary fringe, it becomes irregular, characterized by fingering and more extensive lateral than vertical movement. After spreading ceases, the contaminated area in homogeneous samples consists of two distinct regions: an elongated pancake-shaped oil lens of high NAPL saturation, which extends from the top of the capillary fringe up to the boundary between visibly wet and dry sand, and the area above it, previously swept by the front, at lower kerosene saturation.

b) The ratio of spreading rates during infiltration for the coarse and fine sand (86.95/18.8= 4.6). While the ratio of kerosene of infiltration rates was twice as high (21.6/2.9 =7.4). These results can be explained by considering the different saturation profiles for the two sands.

c) In order to move downward, kerosene has to displace more water in the fine sand than in the coarse sand, as evidenced by the higher saturation changes during infiltration in the fine sand samples and by the larger volume of water displaced at the end of the infiltration stage, 275 cm^3 for the fine sand compared to only 145 cm^3 for the coarse sand.

d) The experiments with homogeneous coarse and fine sands showed that the kerosene infiltrates more rapidly in the coarse sand, however, while vertical movement is delayed in the fine sand, kerosene moves laterally. As a result, although in both cases the kerosene front (from leak source) extends over the same vertical distance 21.7 cm and 22.9 cm for the coarse and fine sand, respectively.

e) The plume moved faster in the coarse sand, as expected. The total contaminated volume was lower, 2655 cm^3 and 3675 cm^3 for the coarse and fine sand, respectively.

f) Decreasing trend of contaminant movement due to the presence of the gypsum content, fine and other soluble salts in Al Najaf city sand caused the reduction in the hydraulic conductivity, consequently, the reduction in the hydraulic conductivity is due to the plugging of soil pores by the precipitation of the leached gypsum.

REFERENCE

- Al Shakerchy, M. S.," Geotechnical Properties of Al Najaf City Soil With Emphasis On Infiltration And Strength Characteristics", A Thesis Submitted To The Building And Construction Engineering Department In The University Of Technology In Partial Fulfillment Of The Requirement For The Degree Of Doctor Of Philosophy In Geotechnical Engineering, 2007.

Bear, J., "Dynamics of fluids in porous media". Elsevier, New York, 1972.

- Das, M. B.," Advance soil mechanics", Mc raw Hill Book Com.,1985.

- Mckee, J. E., F. B. Laverty, and R. M. Hertel, "Gasoline in groundwater". J. Water Pollution Control Fed., 44(2), 293-302, 1972.
- Kramer, W. H., "Ground-water pollution from gasoline", Ground Water Monit. Rev., 2(2), 18-22, 1982.

- Mercer, J.W. and Cohen, R.M. "A review of immiscible fluids in the subsurface: properties, models, characterization and remediation. Journal of contaminant Hydrology, 6:107-163, 1990.

- Oliveira, D. P., and Siter, Groundwater contamination from underground solvent storage tanks", Santa Clara, California, paper presented at 5th National Symposium and Exposition on

Aquifer Restoration and Groundwater Monitoring, Water Well Assoc., Columbus, Ohio, May 21-24, 1985.

- Pantazidou, M., and N. Sitar, "Emplacement Of non-aqueous liquids in the vodase zone". Water Resources Research, 22(1), 25-33, 1993.

- Schwille, F., "Migration of organic fluids immiscible with water, in Pollutants in Porous Media", Ecol. Stud., vol. 47, pp.27-48, Springer-Verlag, New York, 1984.

- Thornton, J. S., Underground movement of gasoline on groundwater and enhanced recovery by surfactants", paper presented at proceedings of the National Conference on Control of Hazardous Material Spills, U.S.Environ. Protect. Agency. Louisivlle, Ky., May 13-15, 1980.

- Watts, R. J., "Hazardous wastes: Sources, Pathways, Receptors". John Wiley, USA, 1998.

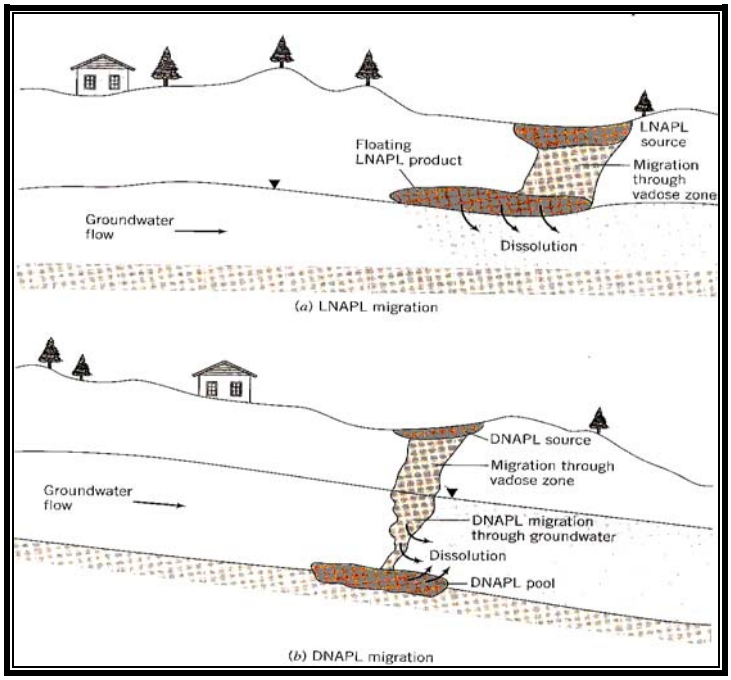

Figure 1: Conceptualized representation of (a) LNAPL and (b) DNAPL migration and contamination of the subsurface (Watts, 1998).

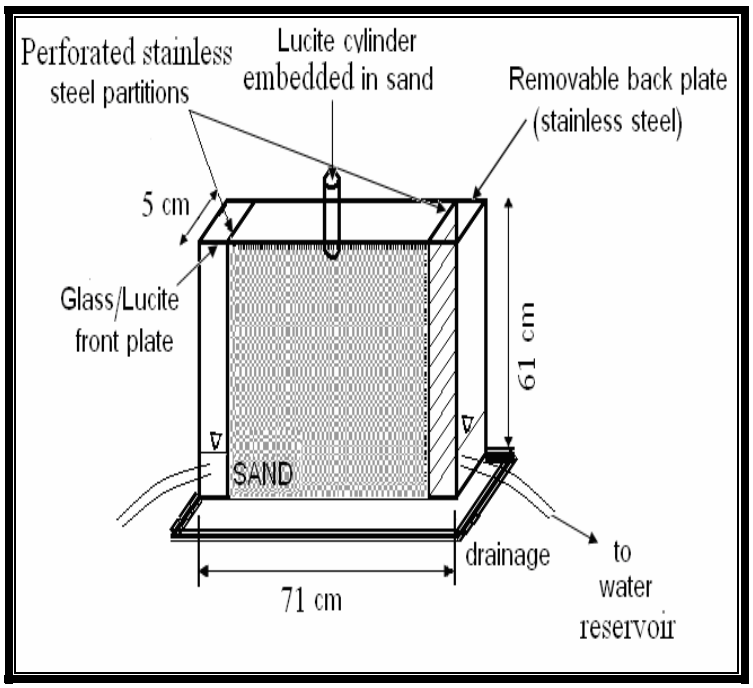

Figure 2: Tank configuration for the sand tank used in the present study.

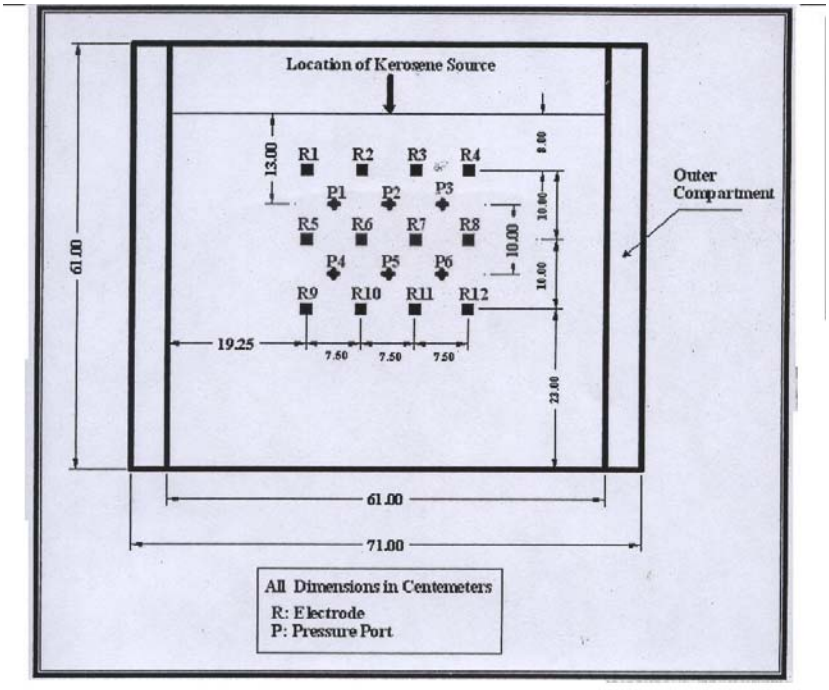

Figure 3: Pressure ports and electrodes locations for the sand tank used in the present study.

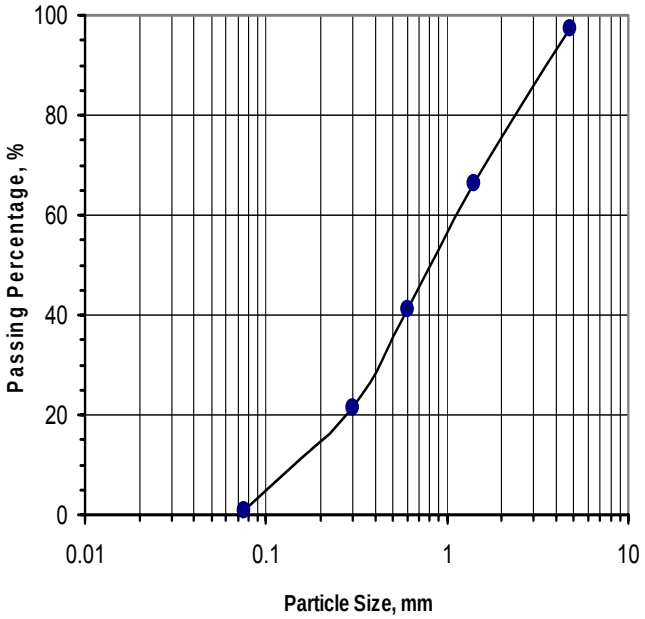

Figure 4: Gradation curve for Al-Najaf city sand.

Table 1: Kerosene properties (Pantazidou and Sitar, 1993).

Parameter	Value
Specific gravity	0.8 at 15 ° C
Viscosity	1.152 CP at 21 ° C
Surface tension: kerosene-air	27.5 dyne/cm at 20 ° C
Interfacial tension: kerosene-water	48 dyne/cm at 20 ° C

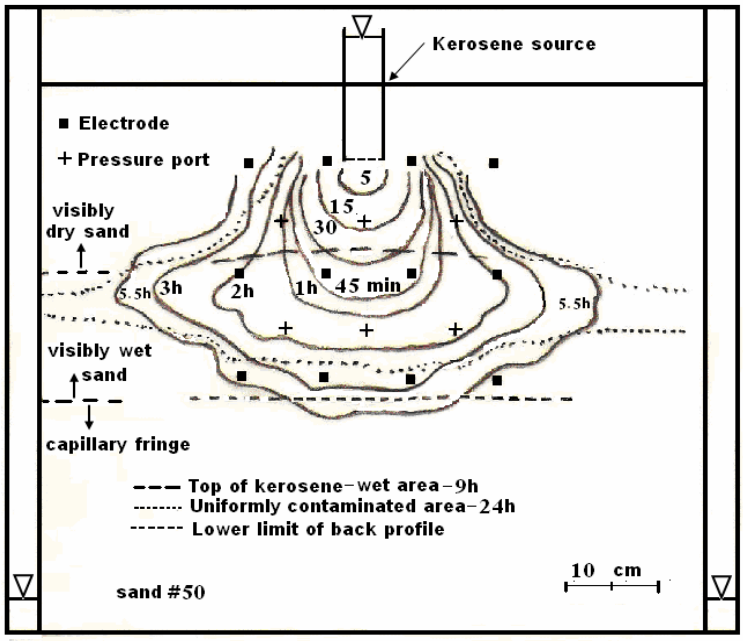

Figure 5: Kerosene front propagation traced during the experiment in the fine sand medium (#50).

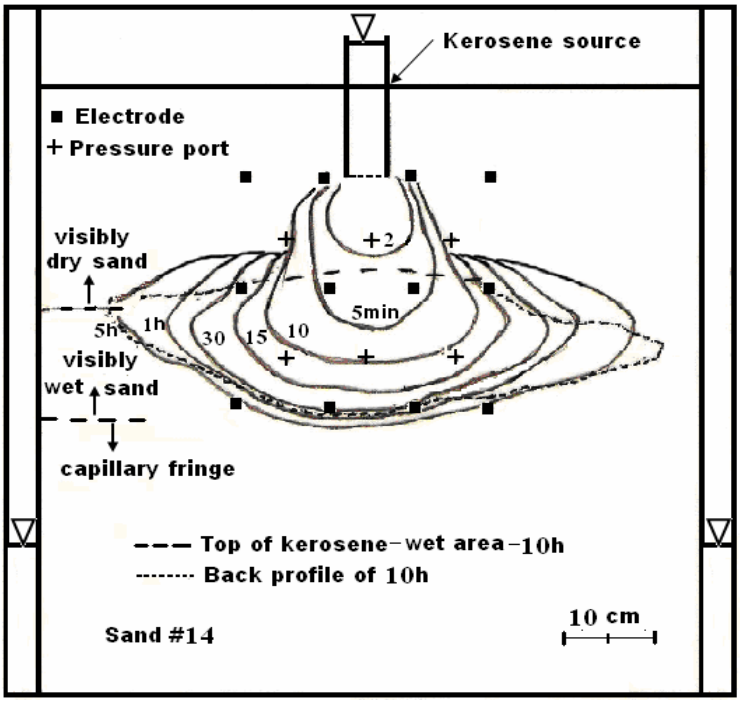

Figure 6: Kerosene front propagation traced during the experiment in the coarse sand medium (#14).

Table 2: Comparison of mean values of front propagation parameters for sands (#14) and (#50).

Time, min	*Type of Sand,#*	*Kerosene Volume, cm^3*	*Contaminated Soil Volume, cm^3*	*Distance from Leak, cm*	*Distance from Water Table, cm*
5	14	107	581	13.1	16.5
	50	-	53	2.7	37.3
10	14	203	1121	17.5	12.4
	50	47	164	4.5	35.4
15	14	350	1718	18.8	10.8
	50	72	262	6.1	33.9
45	14	350	2145	21.2	8.4
	50	135	971	13.5	27.6
Final	14	350	2655	21.7	8.1
	50	350	3675	22.9	17.6

Table 3: Comparison of mean values intervals of final front parameters for sands (#14) and (#50).

Type of Sand	*Lens Thickness, cm*	*Contaminated Soil Volume to Kerosene Volume Ratio*	*Contaminated Soil Volume, %*
#14	11.7	7.59	19.34
#50	16.8	10.50	21.14

Table 4: Summary of two tests of fine and coarse sand.

Type of Sand	*Average Porosity*	*Initial Water Saturation, %*	*Water Table Height, cm*	*Infiltration Duration (Constant Kerosene Head/Total), min*	*Water Displaced at the End of Kerosene Infiltration, cm^3*
Fine sand (#50)	0.44	84.0	3.9	132/150	275
Coarse sand (#14)	0.41	84.5	16.0	10/11	145